Supplement of Atmos. Chem. Phys., 17, 14747–14770, 2017
https://doi.org/10.5194/acp-17-14747-2017-supplement

Atmospheric Chemistry and Physics
Open Access
EGU

Supplement of

Observational assessment of the role of nocturnal residual-layer chemistry in determining daytime surface particulate nitrate concentrations

G. Prabhakar et al.

Correspondence to: Christopher D. Cappa (cdcappa@ucdavis.edu) and Gouri Prabhakar (gourip@ucdavis.edu)

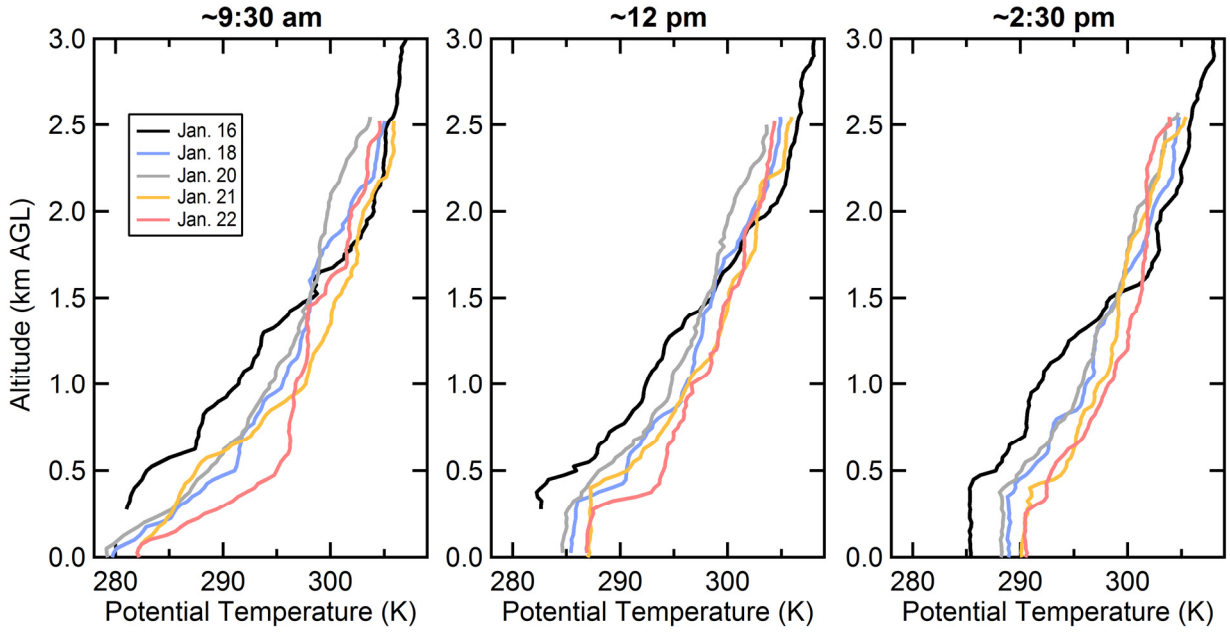

Figure S1. Vertical profiles of potential temperature over Fresno measured by the P-3B for pollution Episode 1 flight days for (left) the morning profile, (middle) the late morning/early afternoon profile and (right) the afternoon profile.

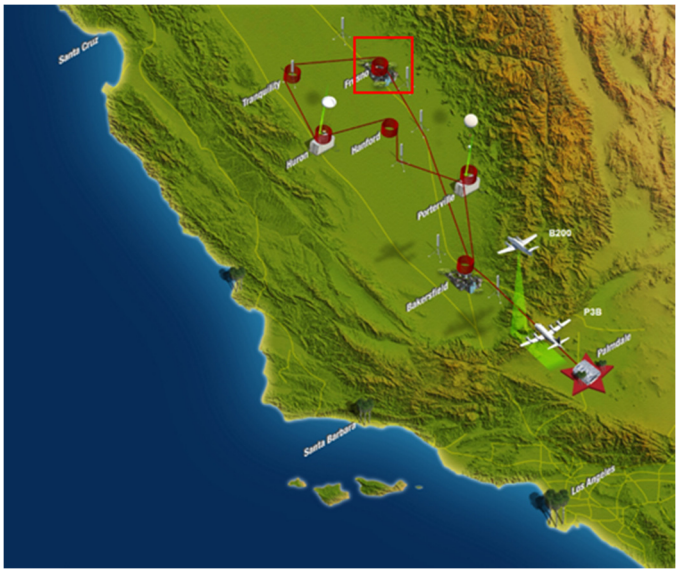

Figure S2. Map of San Joaquin Valley, California showing the flight paths of the P3-B and B200 aircrafts and the location of the six sites over which vertical spirals were done. Image from: http://discover-aq.larc.nasa.gov/multimedia.html. The Fresno site is indicated with a red box.

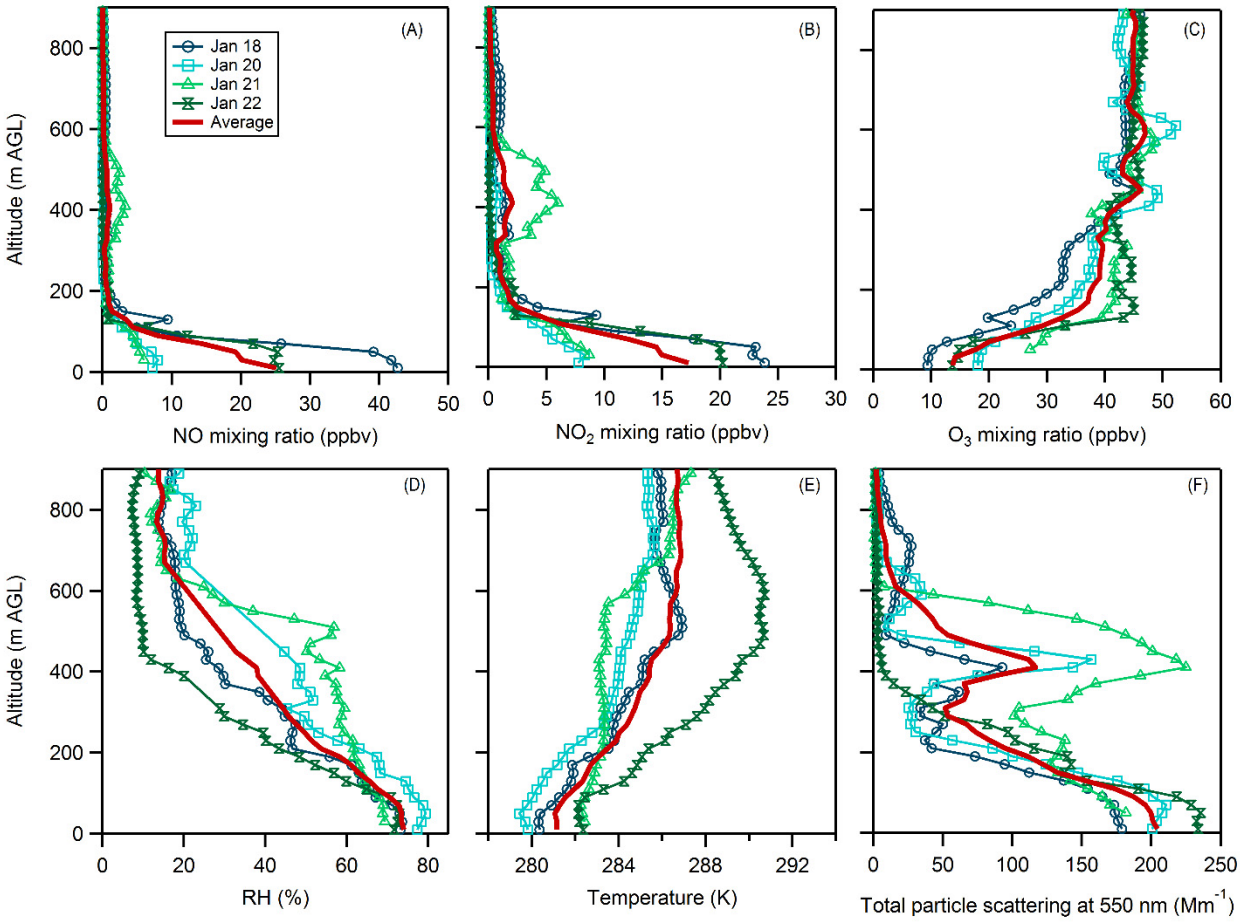

Figure S3. Vertical profiles on individual flight days of (A) NO mixing ratio (ppbv), (B) NO_2 mixing ratio (ppbv), (C) O_3 mixing ratio (ppbv), (D) RH (%), (E) ambient temperature, in K, and (F) total particle scattering at 550 nm in the morning (~9:30 am) over Fresno. Individual days are shown as green and blue and the average as the solid red line.

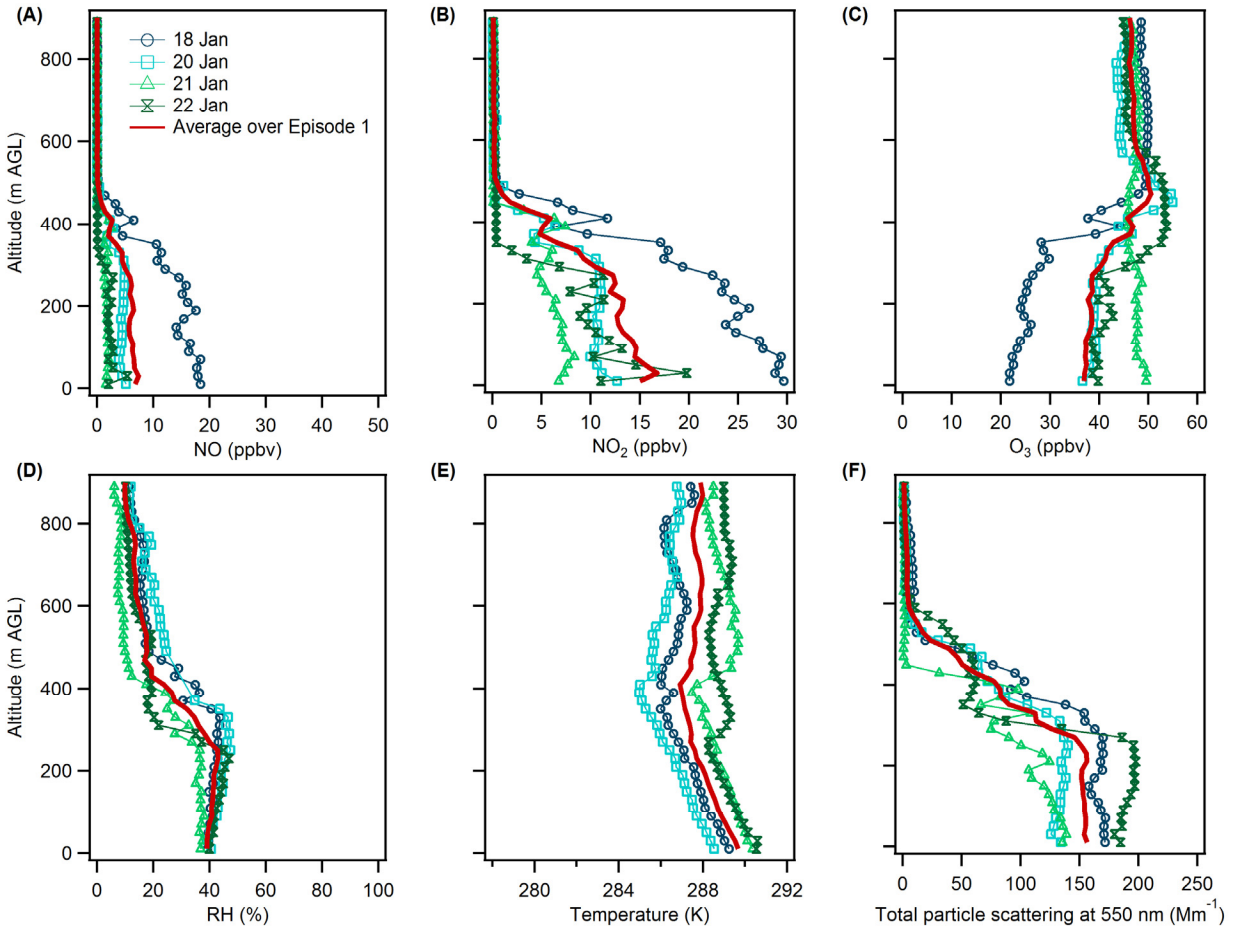

Figure S4. The observed afternoon (2:30 pm) vertical profiles over Fresno on individual flight days during the first episode of: (A) the NO mixing ratio (ppbv); (B) the NO_2 mixing ratio (ppbv); (C) the O_3 mixing ratio (ppbv); (D) relative humidity (%); (E) ambient temperature (K); and (F) the total particle scattering at 550 nm. Individual profiles are shown with symbols and the average profile is shown as a solid red line.

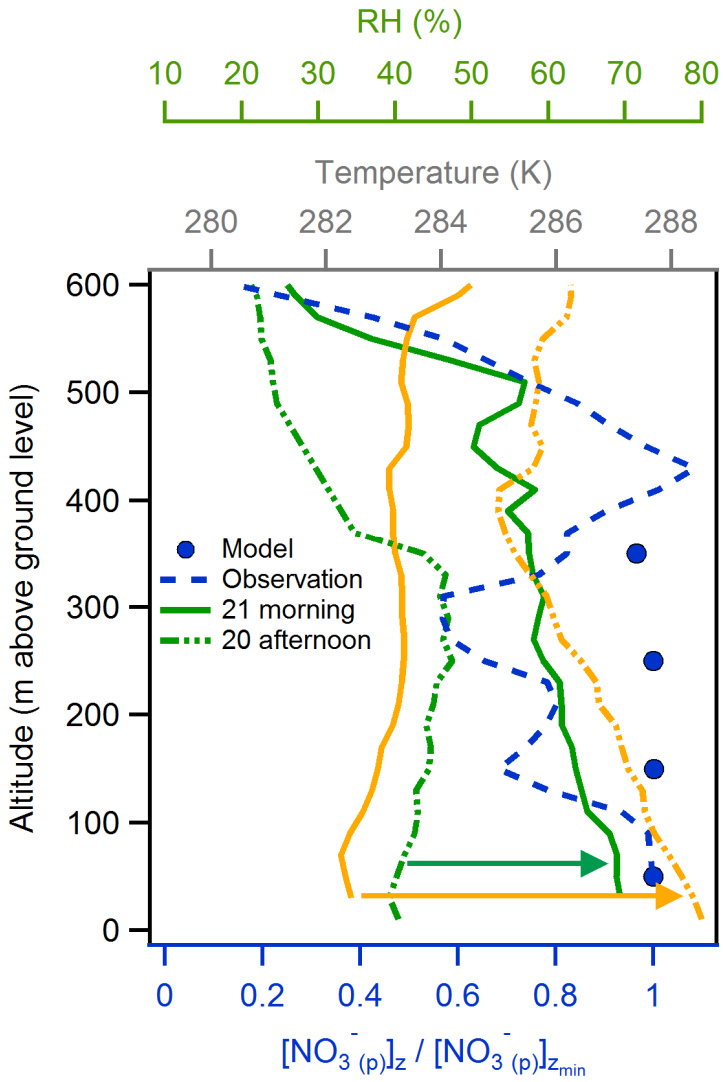

Figure S5. The vertical distribution of the observed normalized $NO_3^-{}_{(p)}$ (dashed blue line) for the first flight leg (early morning) on 21 Jan early morning along with box model prediction of the same (blue dots). (The normalized $NO_3^-{}_{(p)} = [NO_3^-{}_{(p)}]_z/[NO_3^-{}_{(p)}]_{z_{min}}$, where z is altitude and z_{min} is lowest altitude.) Also shown are vertical profiles of temperature (yellow) and relative humidity (green) observed during the third flight leg (afternoon) on 20 Jan (dashed lines) and during the first flight leg (early morning) on 21 Jan morning (solid lines). The horizontal arrows indicate the overnight evolution of temperature and RH.

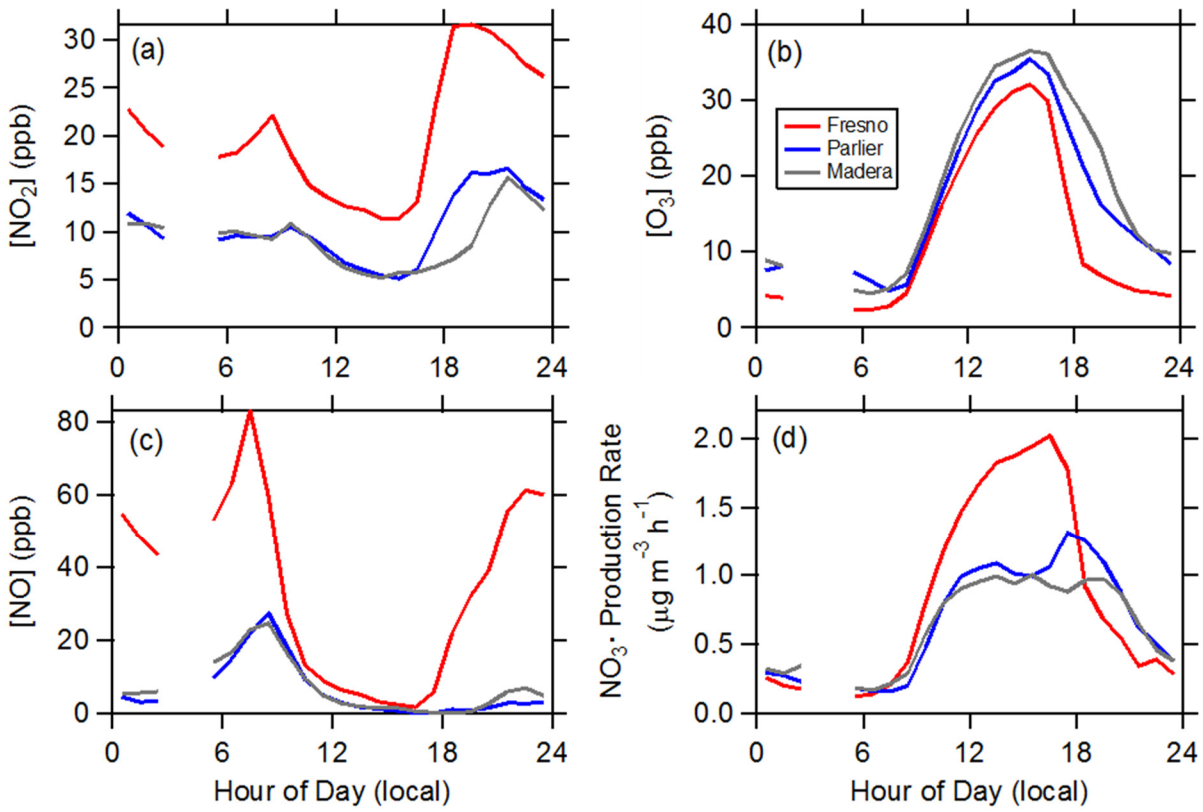

Figure S6. Diurnal profiles of (a) NO_2, (b) O_3, (c) NO and (d) the instantaneous NO_3· production rate for (red) Fresno, (blue) Parlier and (gray) Madera.

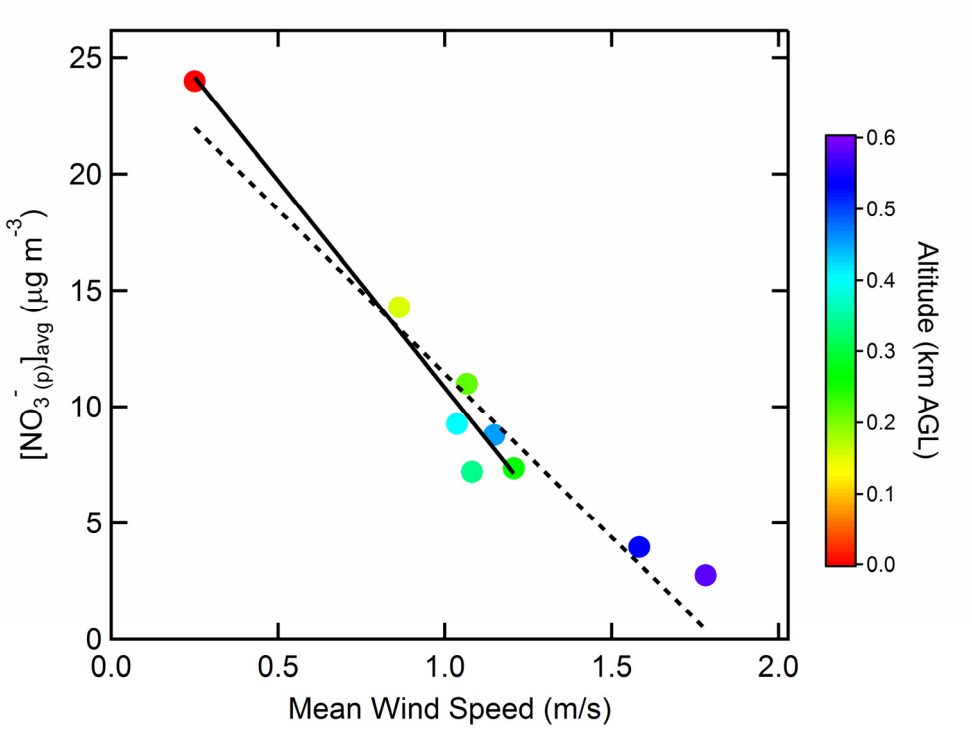

Figure S7. Relationship between the Episode 1 average vertical profiles of estimated $NO_3^{-}{}_{(p)}$ concentrations and the night time mean wind speed. The mean wind speed is for only the nights preceding flight days. Points are colored according to altitude above ground level. The solid black line is a linear fit for altitudes < 0.45 km, with slope = -17.8 µg.s m^{-4} and intercept 28.6 µg m^{-3} and r = -0.98. The dashed black line is a fit to all points below 1 km (r = -0.96).

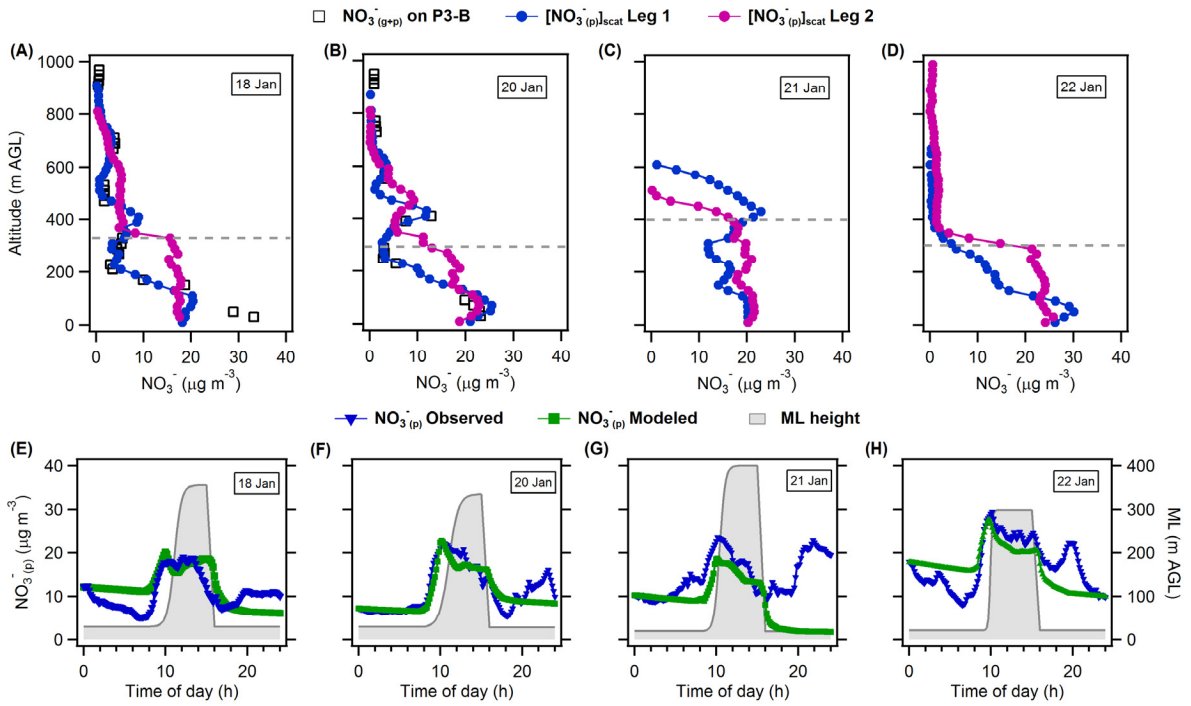

Figure S8. (A-D) The observed vertical profiles of $NO_3^-{}_{(g+p)}$ (black squares) from the TD-LIF and $NO_3^-{}_{(p)}$ (blue circles) for the first flight leg, along with the $NO_3^-{}_{(p)}$ for the second flight leg (purple circles). The horizontal dashed grey lines indicate the ML height at the time of the Fresno profile during flight leg 2. (E-H) The diurnal variation in the observed (blue) and modeled (green) surface-level $NO_3^-{}_{(p)}$ for each flight day in Episode 1. The temporal variation in the BLH (grey shaded area) is shown for reference.

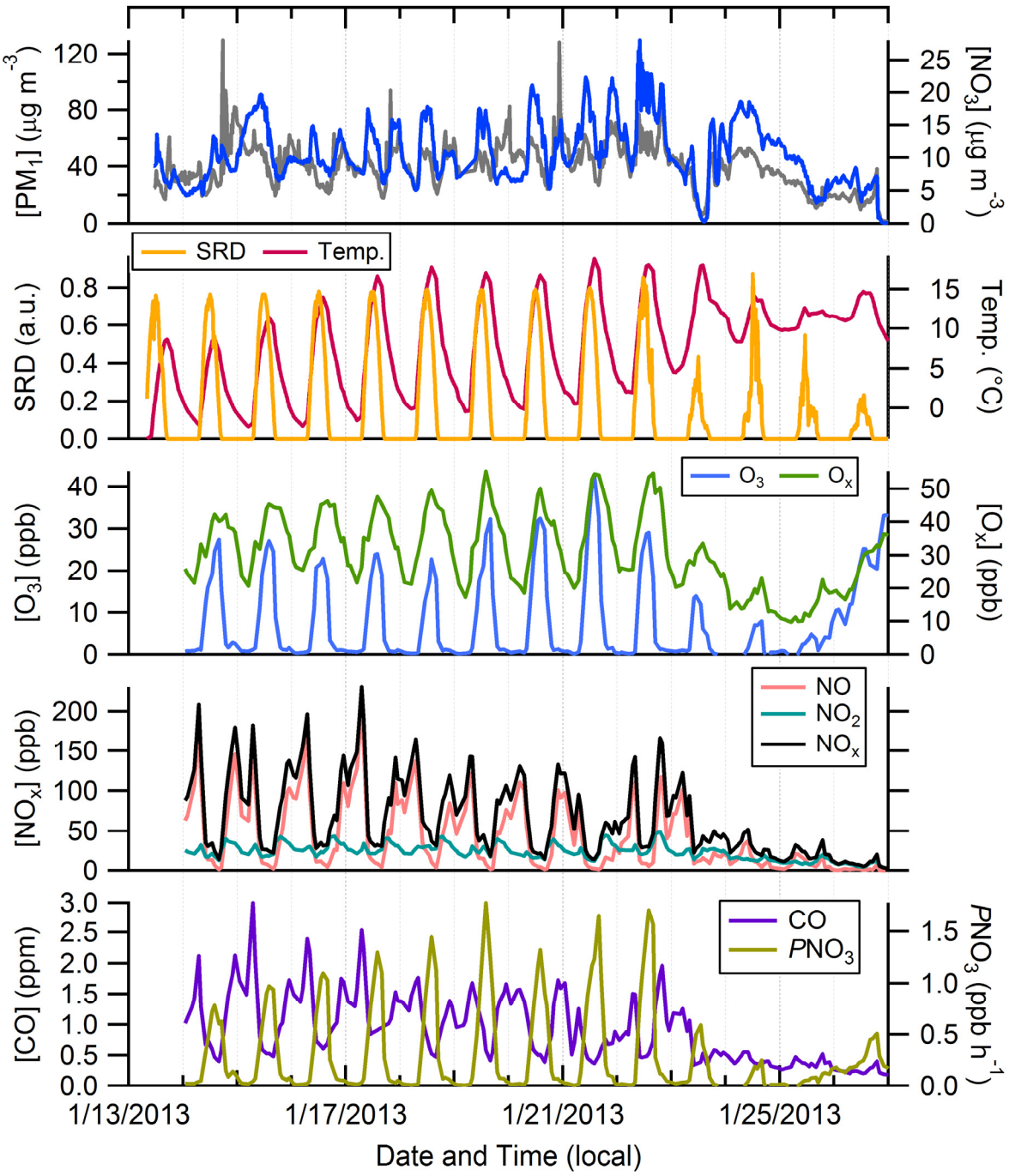

Figure S9. Time-series of observed (top-to-bottom) PM_1 and particulate NO_3^- concentrations, solar radiation (SRD) and temperature, O_3 and O_x concentrations, NO, NO_2 and NO_x concentrations, and CO concentrations with the instantaneous nitrate radical production rate, calculated as $PNO_3 = k_{NO3}[NO_2][O_3]$.

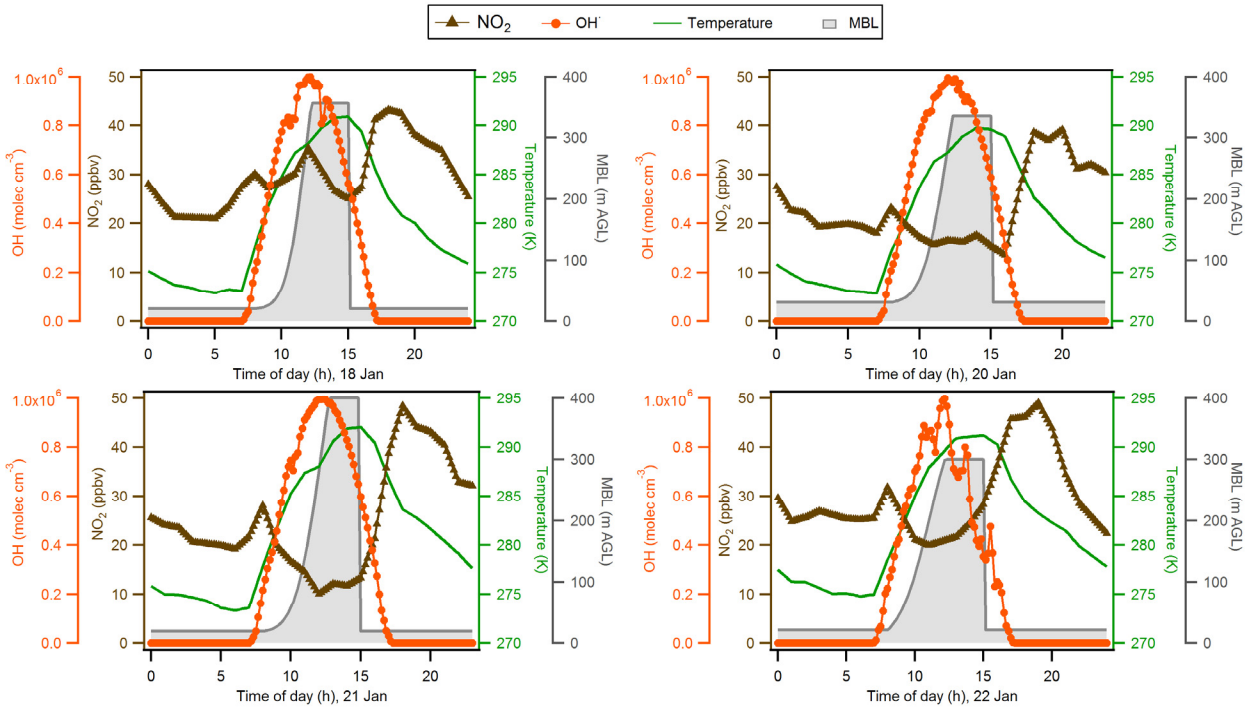

Figure S10. Ground observations of NO_2 (brown triangles) and temperature (green line) and the estimated OH (orange circles) and boundary layer height (gray) that are used to as inputs to the mixing model for each of the four flight days in Episode 1.

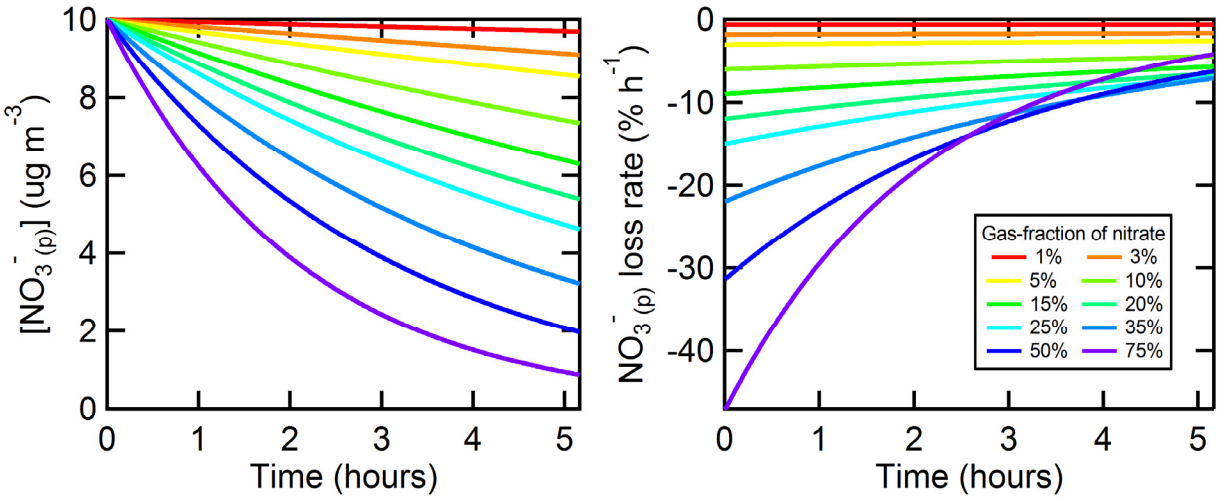

Figure S11. (left) Example model results of the influence of gas-phase HNO_3 deposition on $NO_3^-_{(p)}$ concentrations for different assumed gas-phase nitrate fractions (indicated by color). Here, a constant v_d = 7 cm s^{-1} and mixed-layer height of 400 m are used, and the gas and particles are assumed to remain in equilibrium at all times. The initial $NO_3^-_{(p)}$ concentration is 10 μg m^{-3}. For Fresno, the observed daytime gas-phase nitrate fractions are <10%. (right) The corresponding instantaneous $NO_3^-_{(p)}$ loss rate, in percent. The loss rate is independent of the assumed initial $NO_3^-_{(p)}$ concentration.

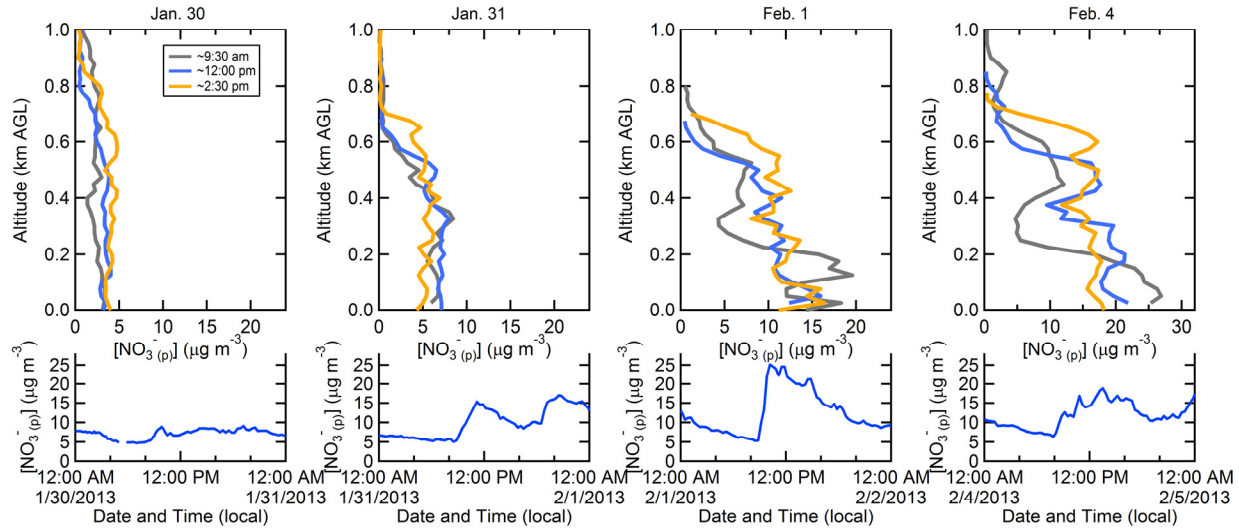

Figure S12. (top row) Vertical profiles of estimated $NO_3^-{}_{(p)}$ concentrations during the flight days in the second episode. The different curves are for individual flight legs. (bottom row) The individual day diurnal variability in the surface $NO_3^-{}_{(p)}$ concentrations for each flight day.

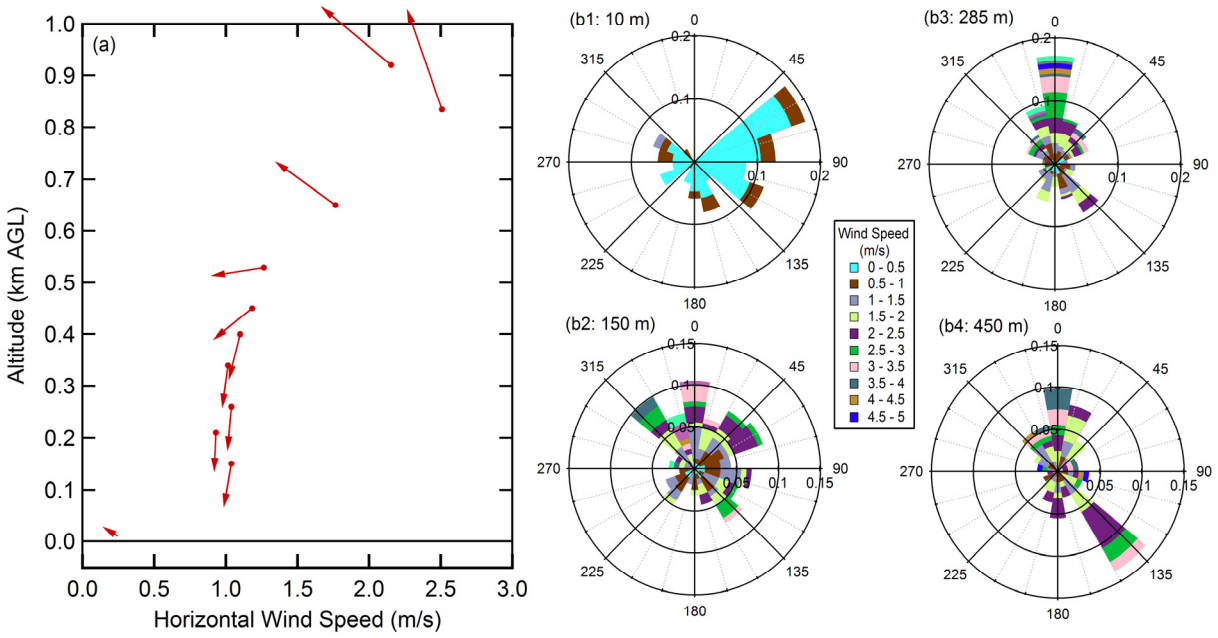

Figure S13. (a) Vertical profile of the average night time (19:00-07:00) horizontal winds over Visalia, CA (65 km SE of Fresno) and the surface (10 m) wind in Fresno during Episode 2 (Jan. 29-Feb. 4). The length of the arrows corresponds to the wind speed and the direction to the average wind direction. (b) Corresponding wind roses for (b1) the surface, (b2) 125-175 m, (b3) 225-345 m, and (b4) 400-500 m. The length of each arc corresponds to the normalized probability and the colors indicate the wind speed (m/s; see legend). Data are from the National Oceanic and Atmospheric Administration, Earth System Research Laboratory, Physical Sciences Division Data and Image Archive (https://www.esrl.noaa.gov/psd/data/obs/datadisplay/, accessed 3 June 2017).

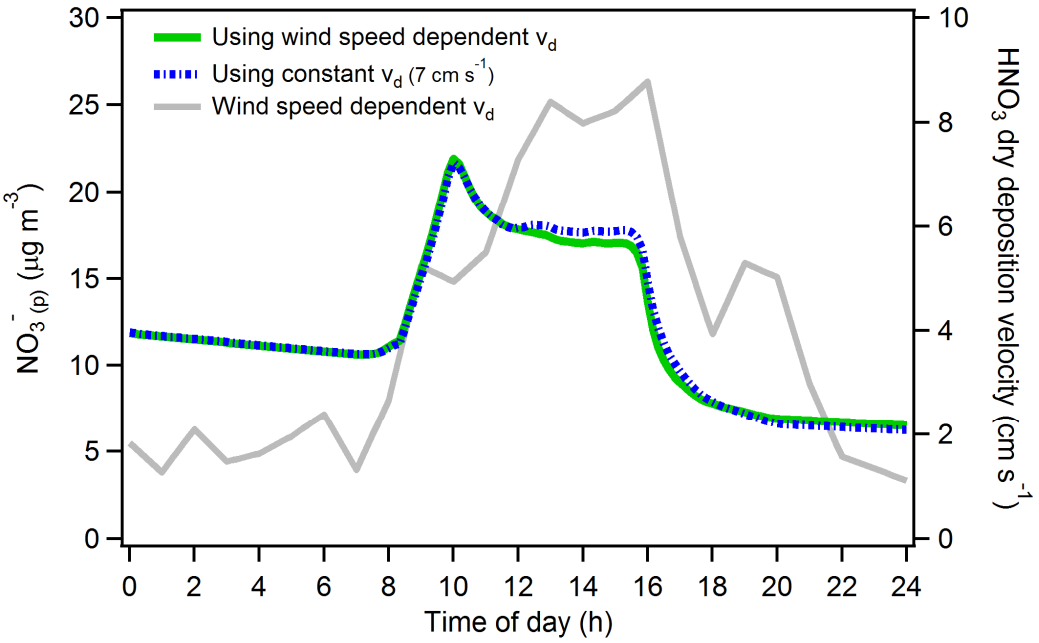

Figure S14. Comparison of model simulations of the averaged diurnal variability in surface-level $NO_3^-{}_{(p)}$ between when the HNO_3 deposition velocity is assumed constant at 7 cm s^{-1} (blue dashed line) and when the deposition velocity varies linearly with surface wind speed (solid green line). The wind-dependent HNO_3 deposition velocity is shown for reference (gray line).

Table S1. Summary of initial conditions measured at the surface-level (3 pm) used for calculation of k_{N2O5} and γ_{N2O5} for flight days during Episode 1.

Dates	NO (ppbv)	NO_2 (ppbv)	O_3 (ppbv)	T (K)	RH (%)	$NO_3^-{}_{(p)}$ (μg m^{-3})	$SO_4^{-2}{}_{(p)}$ (μg m^{-3})	$Cl^-{}_{(p)}$ (μg m^{-3})	$PNO_3^-{}_{(p)}$ (μg m^{-3} nt^{-1})^	S_a (μm^2 cm^{-3})	k_{N2O5} 1E-5 (s^{-1})	γ_{N2O5} 1E-4
17th – 18th Jan	6.3	23.8	23.7	290	31.8	8.5	0.70	0.12*	14.9	525.6	1.6	4.76
19th – 20th Jan	3.7	21.3	31.5	290	36.4	14.3	0.93	0.35	14.4	826.5	1.3	2.46
20th – 21st Jan	2.8	15.4	31.3	290	37.9	11.5	0.90	0.12	10.7	515.5	1.3	3.94
21st -22nd Jan	1.5	13.3	41.7	292	30.0	9.9	1.0	0.01	25.3	295.1	5.1	2.70

* Equal to 1.24 x AMS Cl

^ Overnight particulate nitrate production rate estimated from the difference in the maximum $[NO_3^-{}_{(p)}]$ in the early-morning vertical profile at ~9:30 am and the ground-level $[NO_3^-{}_{(p)}]$ the previous day at 3 pm. The notation nt^{-1} indicates per night.

Table S2. VOC concentrations and reactivity with the NO_3 radical.

VOC	Daytime concentration[a] (ppb)	k_{rxn}[b] (cm^3 $molecules^{-1}$ s^{-1})	Reactivity (s^{-1})
α-Pinene	0.06	6.20E-12	9.34E-03
β-Pinene	0.02	2.60E-12	1.21E-03
i-Butene	0.11	3.50E-13	9.78E-04
Isoprene	0.05	7.00E-13	8.64E-04
DMS[c]	0.01	1.10E-12	2.86E-04
trans-2-Butene	0.03	3.50E-13	3.00E-04
cis-2-Butene	0.03	3.50E-13	2.89E-04
Ethanol[c]	2.45	2.00E-15	1.22E-04
Acetaldehyde[c]	5.14	2.60E-15	3.34E-04
1-3-Butadiene[c]	0.03	1.10E-13	9.17E-05
Propene	0.40	9.40E-15	9.29E-05
Methanol[c]	8.52	1.30E-16	2.77E-05
1-Butene	0.08	1.30E-14	2.54E-05
m-Xylene	0.28	2.30E-15	1.64E-05
o-Xylene	0.20	3.90E-15	1.90E-05
1-Pentene	0.03	1.50E-14	1.04E-05
Propane[c]	4.55	7.00E-17	7.97E-06
Ethene	1.73	2.00E-16	8.65E-06
1-2-4-Trimethylbenzene	0.09	1.72E-15	3.81E-06
Ethyne	1.81	1.00E-16	4.53E-06
Others[c]	0.29	2.1E-17	1.52E-07

[a]From canister samples, averaged for the afternoon period
[b]From Calvert et al., *The Mechanisms of Reactions Influencing Atmospheric Ozone*, Oxford University Press, 2015, pp. 130-160.
[c]These VOCs are assumed to react with NO_3 radicals to form HNO_3.